



저작자표시-비영리-변경금지 2.0 대한민국

이용자는 아래의 조건을 따르는 경우에 한하여 자유롭게

- 이 저작물을 복제, 배포, 전송, 전시, 공연 및 방송할 수 있습니다.

다음과 같은 조건을 따라야 합니다:



저작자표시. 귀하는 원저작자를 표시하여야 합니다.



비영리. 귀하는 이 저작물을 영리 목적으로 이용할 수 없습니다.



변경금지. 귀하는 이 저작물을 개작, 변형 또는 가공할 수 없습니다.

- 귀하는, 이 저작물의 재이용이나 배포의 경우, 이 저작물에 적용된 이용허락조건을 명확하게 나타내어야 합니다.
- 저작권자로부터 별도의 허가를 받으면 이러한 조건들은 적용되지 않습니다.

저작권법에 따른 이용자의 권리는 위의 내용에 의하여 영향을 받지 않습니다.

이것은 [이용허락규약\(Legal Code\)](#)을 이해하기 쉽게 요약한 것입니다.

[Disclaimer](#)

Thesis for the Degree of Master of Science

**A Study on Urban Parameterization**  
**Using GIS and CFD model**



by

Lee Hankyung

Department of Environmental Atmospheric Sciences

The Graduate school

Pukyong National University

February 2016

# A Study on Urban Parameterization

Using GIS and CFD model

(GIS 와 CFD 모델을 이용한  
도시 모수화에 관한 연구)

Advisor: Prof. Jae-Jin Kim

by

Lee Hankyung

A thesis submitted in partial fulfillment of the requirements  
for the degree of

Master of Science

in Department of Environmental Atmospheric Sciences, the Graduate School

Pukyong National University

February 2016

# A Study on Urban Parameterization Using GIS and CFD model

A dissertation

by

Lee Hankyung

Approved by:



(Chairman)

Hyeong-Bin Cheong



(Member)

Won-Sic Choi



(Member)

Jae-Jin Kim

February 26, 2016

# Contents

List of Figures .....	v
List of Tables.....	vi
Abstract .....	vii
1. Introduction .....	1
2. Methodology.....	5
2.1. CFD model .....	5
2.2. GIS data .....	6
2.3. Experimental setup .....	7
2.3.1. Simplified building group.....	7
2.3.2. Real area .....	13
3. Results and discussions .....	16
3.1. Simplified building group.....	16
3.1.1. Analysis on the change region by building group .....	16
3.1.2. Parameterization for wind speed within building group .....	20
3.2. Real area.....	26
3.2.1. Correlations between bulk geometric parameters and wind speed.....	26
3.2.2. Roughness length and zero plane displacement height.....	33
3.2.3. Correlation among effective roughness height and bulk geometric parameters.....	38

4. Summary and conclusions ..... 42

REFERENCE ..... 45



# List of Figures

<b>Fig. 1.</b> Numerical domain and building configuration in the control-run (CNTL) case. ....	11
<b>Fig. 2.</b> The numerical simulation results of (a) before and (b) after using fully-developed profile for control-run at $z = 0.05H$ . ....	12
<b>Fig. 3.</b> An example (Gangnam area in Seoul) of two-dimensional building configurations of 30 target areas. Bulk geometric parameters are calculated in the upwind region within the dashed lines in (a) and statistics for wind are taken in the downwind region within blue colored area in (b). Bold arrows indicate inflow direction. ....	15
<b>Fig. 4.</b> Isosurface for the 10% reduction region of wind component in the x-direction ( $U$ ) in each case. ....	18
<b>Fig. 5.</b> (a) total volume of the reduction region in $U$ -vector normalized by the building volume in the CNTL case and (b) $U$ -vector reduced area fraction normalized by the plane area of the building in the CNTL case. ....	19
<b>Fig. 6.</b> The vertical profiles of the wind speed in the x-direction ( $ U $ ) averaged within the buildings. ....	23
<b>Fig. 7.</b> The wind speed averaged within the buildings with the inflow speed and plane area fraction ( $\lambda_p$ ). ....	24
<b>Fig. 8.</b> Wind speed calculated by the parameterization method versus simulated by the CFD model using GIS data for 80 target areas selected in 7 cities in	

Korea.....	25
<b>Fig. 9.</b> The correlation between (a) $\sigma_H$ and $H_{ave}$ , (b) $\sigma_H$ and $H_{max}$ , (c) $\lambda_f$ and $\lambda_p$ . .....	28
<b>Fig. 10.</b> (a) The domain of gang-nam in Seoul and (b) the variation of wind speed at $z = 2.5$ m with building height.....	31
<b>Fig. 11.</b> The ratio of average wind speed at 12.5 m and 195.0 m over the central area to inflow speed with (a) $H_{ave}$ , (b) $H_{max}$ , (c) $\lambda_p$ and (d) $\lambda_f$ . The average building height of 120 districts is 12.5 m and the tallest building height considered in this study is 195.0 m.....	32
<b>Fig. 12.</b> The roughness length ( $z_0$ ) and zero plane displacement height ( $d$ ) of urban canopy layer. ....	36
<b>Fig. 13.</b> Vertical average momentum flux and effective roughness height for three urban type. The averaged momentum flux (a) and Seoul (b), Busan (c), Gochang (d) as representative area of each type. ....	37
<b>Fig. 14.</b> The correlation between (a) $z_0$ and $\lambda_p$ , (b) $d$ and $\lambda_p$ , (c) $z_0$ and $\lambda_f$ and (d) $d$ and $\lambda_f$ .....	40
<b>Fig. 15.</b> The correlation between (a) $z_0$ and $\lambda_{vol}$ , (b) $d$ and $\lambda_{vol}$ . ....	41

## List of Tables

<b>Table 1.</b> Summary of the numerical experiments.....	10
---	----



# GIS 와 CFD 모델을 이용한 도시 모수화에 관한 연구

이한경

부경대학교 대학원 환경대기과학과

## 요 약

본 연구에서는 GIS 와 CFD 모델을 이용하여 도시 모수화에 관한 두 가지 연구를 수행하였다. 첫 번째 연구의 목적은 실제 도시 지역에 적용 가능한 풍속 모수화 수식을 도출하는 것이며, 두 번째 연구의 목적은 중규모 기상 모델에서 도시의 건물 효과를 반영할 수 있는 매개변수를 도출하는 것이다. 먼저 첫 번째 연구에서는 CFD 모델을 이용하여 건물 부피비 변화가 건물군 주변과 내부 흐름에 미치는 영향을 조사하였다. 건물 부피비에 따른 건물군 주변과 내부의 흐름 특성을 분석하기 위하여, 일정한 공간 내에서 건물 높이는 고정시키고 부피비를 체계적으로 변화시켜 수치 모의하였다. 건물 부피비가 증가할수록 건물군 주변에 영향을 미치는 영역은 넓게 나타났으며, 이는 건물 규모가 커질수록 넓은 지역에서 흐름에 영향을 미친다는 것을 의미한다. 건물군 내부에서는 건물 부피비가 증가할수록 평균 풍속이 감소하였다. 건물군 내부의 평균 풍속을 건물 부피비와 배경 풍속으로 모수화하였다. 모수화 방법을 GIS 를 이용하여 얻은 7개 도시 80개 지역에서 수치 모의한 결과와 비교하였고, 이 방법이 도시 지역의 평균 풍속을 비교적 잘 모수화하는 것을 확인할 수 있었다. 두 번째 연구에서는 GIS 를 이용하여 얻은 실제 도시 지역 120개 지역을 대상으로 건물의 기하학적 매개변수를 산출하고, CFD 모델로 수치모의를 수행하였다. 건물의 기하학적 매개변수들의 상관관계를 이용하여 지역별 건물의 특성을 알 수 있다. 각 지역별 풍하측 지역의 풍속 저감율과 매개변수들의 관계를 분석해보면, 건물의 옆면비가 풍속과 가장 큰 상관도를 보였다. 기하학적 매개변수를 이용하여 각 지역별 거칠기 길이와 영면변위를 산출한 후, 건물의 평면비와 옆면비와 비교하였다. 거칠기 길이와 영면변위는 풍속과 가장 상관도가 높았던 건물의 옆면비와 양의 상관관계를 나타냈지만, 높은 상관도를 보이지는 않았다. 반면, 건물의 평면비와 옆면비를 모두 반영할 수 있는 건물의 부피비와 높은 상관도를 나타냈다.

# 1. Introduction

Urban areas are composed mainly of many buildings and their surface conditions are clearly distinguished from non-constructed areas such as forest and grass areas (Lee *et al.*, 2011). Building is most important external forcing for wind, temperature and turbulence in urban areas (Brown and Williams, 1998). Hence, flow and pollutant dispersion patterns in urban areas are significantly complicated. People became interested more salubrious circumstances, which motivated many studies on urban flow and dispersion (Britter and Hanna, 2003). There are marked localities in flow and pollutant dispersion patterns in urban areas, depending on building configurations (Kastner-Klein *et al.*, 2004). Also, meteorological elements such as wind speed and direction, momentum and heat fluxes, and so on above urban canopies are much affected by buildings and topography near ground surface (Ohashi *et al.*, 2007). Recently, studies on the flow and diffusion of real urban area have been proceeding based on the geographic information system (GIS) (Chu *et al.*, 2005; Neofytou *et al.*, 2008; Zheng *et al.*, 2010; Toparlak *et al.*, 2015). According to these studies, the buildings act

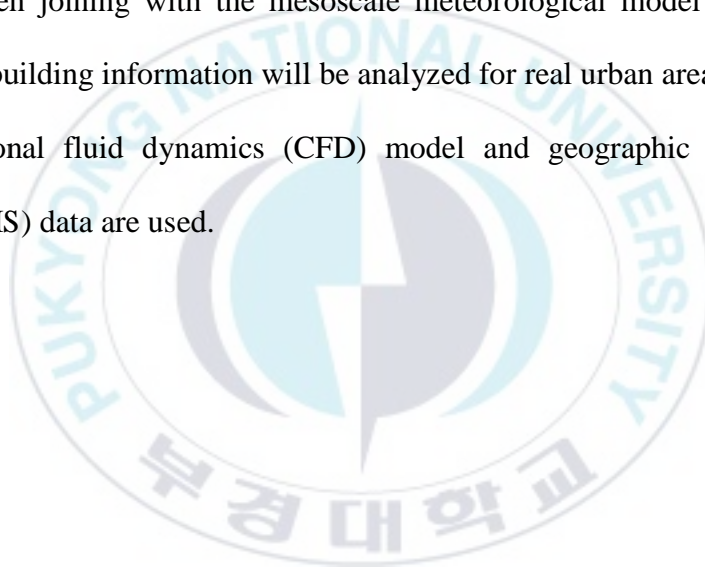
as roughness causing drag effect and reducing wind speed on nearby area of building. In addition, it makes channeling effect of increasing partially wind speed between buildings (Lee *et al.*, 2009).

Despite recent advances in the state-of-the-art computing system, it is impossible to directly simulate the building-scale meteorological phenomena in operating numerical weather prediction system at present. Currently operated local-scale meteorological models have the horizontal resolution of about 1.5 km and, however, it is still larger to resolve meteorological phenomena in urban areas (Byon *et al.*, 2010; Gross, 2014). Instead of direct simulation considering buildings and topography, urban parameterization has been established for taking urban effects into account (Kanda *et al.*, 2013; Santiago *et al.*, 2013). For reflecting urban effects into a weather prediction modeling system, meteorological elements representing urban flow characteristics are parameterized in terms of detailed building or topographic information in urban areas (Grimmond *et al.*, 1998). Roughness length and zero plane displacement height well reflect surface characteristics (Arya, 2001). Macdonald (1998) established roughness length and zero plane displacement height formulated in aerodynamic parameters based on wind-tunnel experiments. Using large-eddy-simulation (LES) results, Kanda *et al.* (2013) suggested modified formulas for roughness length and zero plane

displacement height expressed in urban parameters such as plane area fraction of buildings, averaged building height, maximum building height, standard deviation of building height in urban areas. The roughness length and zero plane displacement height calculated by Kanda *et al.* (2013)'s formulas are quite well correlated with the measured data.

Classification of urban areas into distinct types morphologically is very difficult because urban areas have been atypically constructed according to cultural and regional characteristics (Bhagat, 2005; Lu and Weng, 2006). Nevertheless, in a view of urban parameterization, it is convenient to characterize urban types in terms of building density and height as intensely developed urban area with high-rise buildings, low density urban area with low buildings, and rural area with scattered houses (Oke, 2006). Different urban types have different aerodynamic parameters (Tewari *et al.*, 2008; Lee *et al.*, 2009). Therefore, development of urban parameterization considering aerodynamic parameters adequate for different urban types is required. Estimating morphological parameter of buildings in urban areas, plane area fraction and frontal area fraction are also very important factor (Macdonald *et al.*, 1998; Burian *et al.*, 2007). In order to analyze parameterization scheme reflecting realistic building shape, the volumetric ratio of building that can take into account all of the plane and frontal area fraction is used in this study.

In this paper, two experiments will be analyzed. The first is the development of parameter that can predict wind speed inside the building group using building information only. In targeting uniformly arrayed building, the average wind speed of inside building group will be parameterized by using plane area fraction and inflow profile. The second is the development of parameter that can improve the numerical results of CFD model when joining with the mesoscale meteorological model henceforth. Here, the building information will be analyzed for real urban area. For this, a computational fluid dynamics (CFD) model and geographic information system (GIS) data are used.



## 2. Methodology

### 2.1. CFD model

The CFD model used in this study is the same as Kim *et al.* (2014). The CFD model is based on the Reynolds Averaged Navier–Stokes equations (RANS), assuming a three–dimensional, non–hydrostatic, non–rotating, and incompressible airflow system. A RNG  $k$ – $\epsilon$  turbulence closure scheme is employed for turbulence parameterization. The governing equations are numerically solved on a staggered grid system using a finite volume method and semi–implicit method for pressure–linked equation (SIMPLE) algorithm. The CFD model that was recently improved reproduces very well the experimental wind tunnel results for street–canyon flows (Kim, 2007; Kim and Baik, 2010).

## 2.2. GIS data

In this study, 30 urban areas in Korea are considered as target areas. The target areas include commercial area (5 in Seoul, 2 in Busan and 1 in Daegu), residential and apartment area (3 in Seoul, 2 in Daegu and each 1 in Busan, Daejeon, Jeonju, Ulsan, Gwangju, Pyeongtaek, and Gangneung), industrial area (2 in Deagu, each 1 in Changwon and Dangjin), and rural area (2 in Gangneung and each 1 in Gochang, Chuncheon, Boseong and Gumi). For each target area, geographic information system (GIS) is used in order to construct realistic buildings which are used as ground–surface boundary input data in the numerical model. For purely focusing on the building effect, local topography is ignored as in Kanda *et al.* (2013). These areas are divided into 4 zones of sizes of 1 km × 1 km and area analyzed for a total of 120 regions. Of that, 80 areas of Seoul, Busan, Deagu, Gwangju, Daejeon, Ulsan, Jeonju where buildings relatively are many distributed are used as verification data for the first study. And all data of 120 areas are analyzed as subject of second study.

## 2.3. Experimental setup

### 2.3.1. Simplified building group

COST (European Cooperation in the field of Scientific and Technical Research) recommends that the inlet, lateral and top boundaries should be  $5H$  away for group buildings, where  $H$  is the maximum height. The outflow boundary should be placed over  $10H$  away from the buildings (Franke *et al.*, 2011). Then, the numerical domain was set to meet recommendations of COST. The sizes are 720 m in the x-direction and 520 m in the y-direction, and 200 m in the z-direction with 2 m of the grid size respectively (Fig. 1). There is a space 100 m in x-direction, 100 m in y-direction, 20 m in z-direction for building is located. It is considered as change of volumetric ratio ( $= 0.2, 0.4, 0.6, 0.8, 1.0$ ) (Table 1). The plane area fraction ( $\lambda_p$ ) of building is ratio of the plane area occupied by buildings to plane area in control case (Kanda *et al.*, 2013). The volumetric ratio and plane area fraction of buildings are 1.0 for control case. The building height is constant as 20 m, the volumetric ratio of EXP1 is 0.2 compared with control case.

It is possible to define fully-developed profile when initial inflow is no longer changed within domain. In order to use fully developed profile as

initial boundary condition, the CFD model is integrated in numerical domain except obstacles for 3600s with time step of 1 s. Inflow boundary condition, turbulent kinetic energy and its dissipation rate are specified as

$$U(z) = \frac{U_*}{\kappa} \ln\left(\frac{z}{z_0}\right), \quad (1)$$

$$V(z) = 0, \quad (2)$$

$$W(z) = 0, \quad (3)$$

$$k(z) = \frac{1}{C_\mu^{1/2}} U_*^2 \left(1 - \frac{z}{\delta}\right)^2, \quad (4)$$

$$\varepsilon(z) = \frac{C_\mu^{3/4} k^{3/2}}{\kappa z}. \quad (5)$$

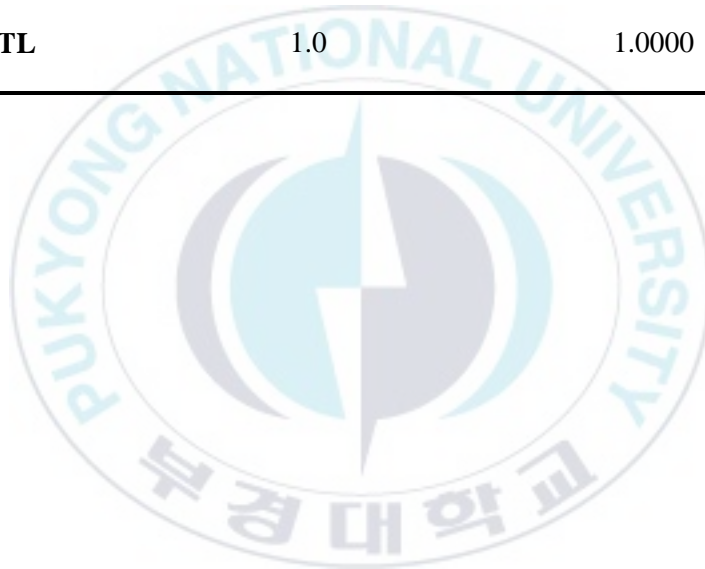
Here,  $U_*$ ,  $z_0$ ,  $\delta$  and  $\kappa$  are the friction velocity, roughness length (= 0.05 m), boundary layer depth (= 1000 m) and von Karman constant (= 0.4) respectively. After the CFD model was integrated for 3600s by using eq. (1)—(5) as initial condition, fully developed wind, turbulent kinetic energy and its dissipation rate that are used as initial boundary data of numerical experiment is obtained. By performing these steps, it is possible to blocking the change of initial inflow profile. Furthermore, when investigating the change in flow by building in downwind areas, the flow changes generated

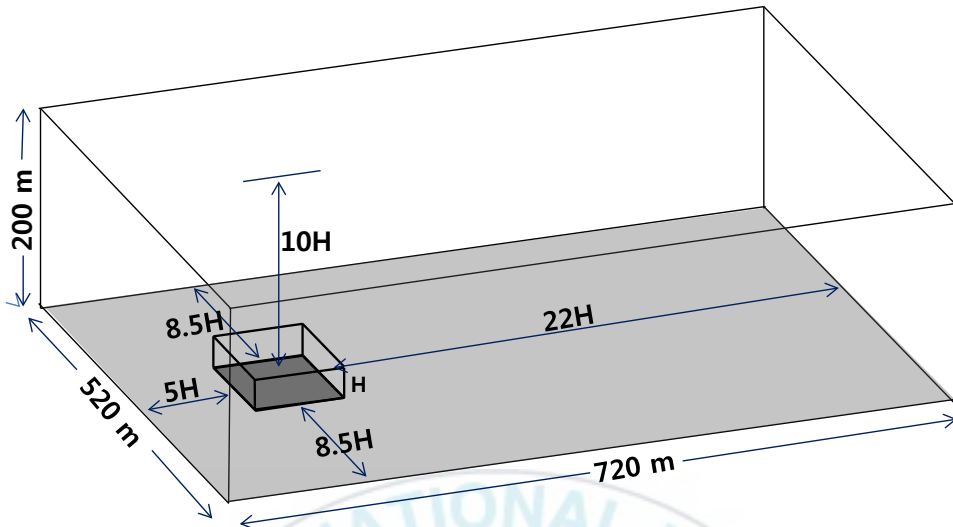
by development process of inflow profile can be eliminated. Figure 2 represent results of before and after using fully-developed profile. It is possible to analyze only the change of wind by building in Figure 2b. In order to investigate the change in wind speed within building group, the initial inflow profile is changed from  $1.5 \text{ m s}^{-1}$  to  $9 \text{ m s}^{-1}$  in  $1.5 \text{ m s}^{-1}$  of the interval roughly at building height.



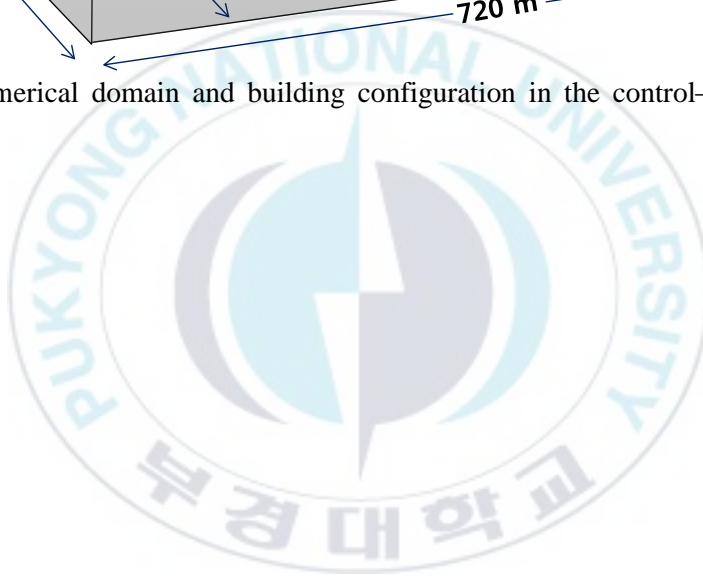
**Table 1.** Summary of the numerical experiments.

experiments	Volumetric ratio	Plane area ratio ( $\lambda_p$ )
<b>EXP1</b>	0.2	0.1600
<b>EXP2</b>	0.4	0.4096
<b>EXP3</b>	0.6	0.5184
<b>EXP4</b>	0.8	0.7744
<b>CNTL</b>	1.0	1.0000





**Fig. 1.** Numerical domain and building configuration in the control-run (CNTL) case.



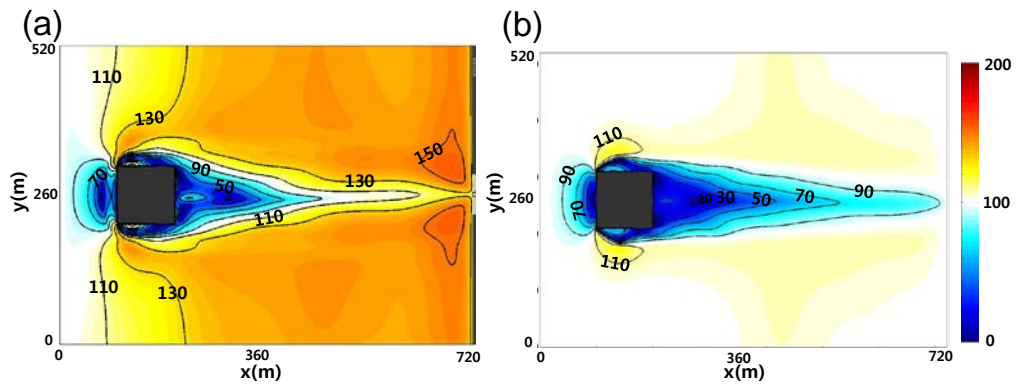
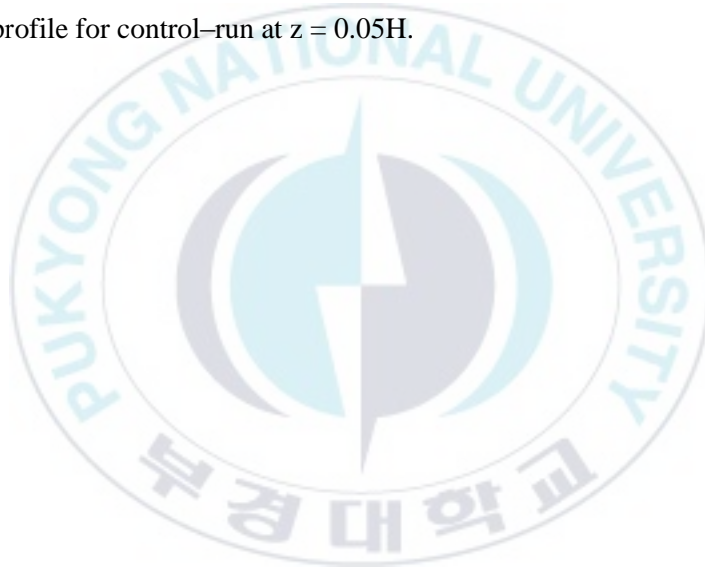


**Fig. 2.** The numerical simulation results of (a) before and (b) after using fully-developed profile for control-run at  $z = 0.05H$ .



### 2.3.2. Real area

For 30 urban areas, we set up the numerical domain with the sizes of 2 km in the x–(east–west) direction and 2 km in the y–(south–north) direction, and 0.75 km in the z–(vertical) direction. The grid sizes are 10 m, 10 m, and 5 m in the x–, y–, and z–directions, respectively. At the inflow boundary, wind, turbulent kinetic energy (TKE), and TKE dissipation rate are specified as

$$U(z) = \frac{U_*}{\kappa} \ln \left( \frac{z}{z_0} \right) \cos \theta, \quad (6)$$

$$V(z) = \frac{U_*}{\kappa} \ln \left( \frac{z}{z_0} \right) \sin \theta, \quad (7)$$

$$W(z) = 0, \quad (8)$$

$$k(z) = \frac{1}{C_\mu^{1/2}} U_*^2 \left( 1 - \frac{z}{\delta} \right)^2, \quad (9)$$

$$\varepsilon(z) = \frac{C_\mu^{3/4} k^{3/2}}{\kappa z}. \quad (10)$$

Here,  $\theta$ ,  $U_*$ ,  $z_0$ ,  $\delta$  and  $\kappa$  indicate the wind direction, friction velocity, roughness length (= 0.05 m), boundary layer depth (= 1000 m) and von Karman constant (= 0.4), respectively. The CFD model is integrated up to

3600 s with time step of 2 s. To investigate the effects of buildings on wind speed in the downwind region, bulk geometric parameters are calculated in the upwind region with the sizes of 1 km  $\times$  1 km (areas in the dashed lines in Fig. 3a) and statistics for wind are taken in the central area (blue colored area in Fig. 3b). Four inflow directions ( $\theta = 0^\circ, 90^\circ, 180^\circ,$  and  $270^\circ$ ) are considered for each target area and, therefore, totally 120 cases are analyzed.



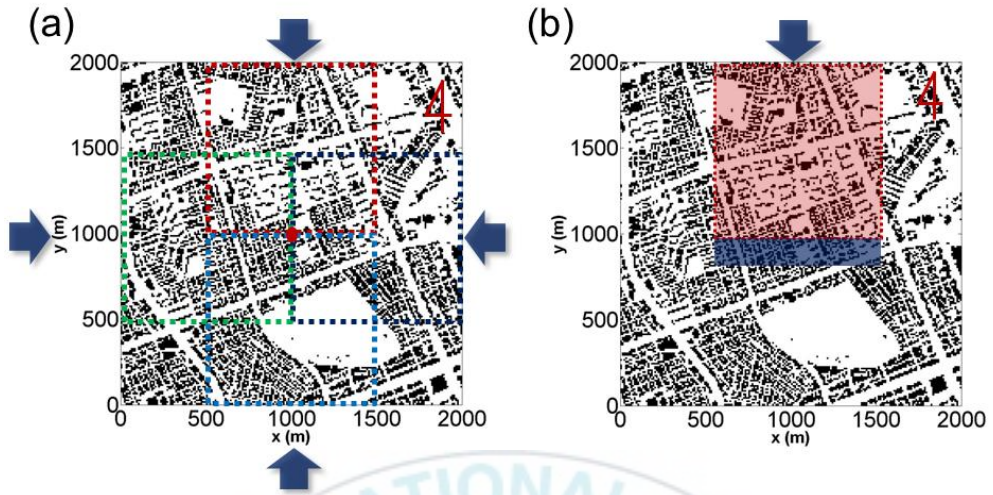


**Fig. 3.** An example (Gangnam area in Seoul) of two-dimensional building configurations of 30 target areas. Bulk geometric parameters are calculated in the upwind region within the dashed lines in (a) and statistics for wind are taken in the downwind region within blue colored area in (b). Bold arrows indicate inflow direction.

## **3. Results and discussions**

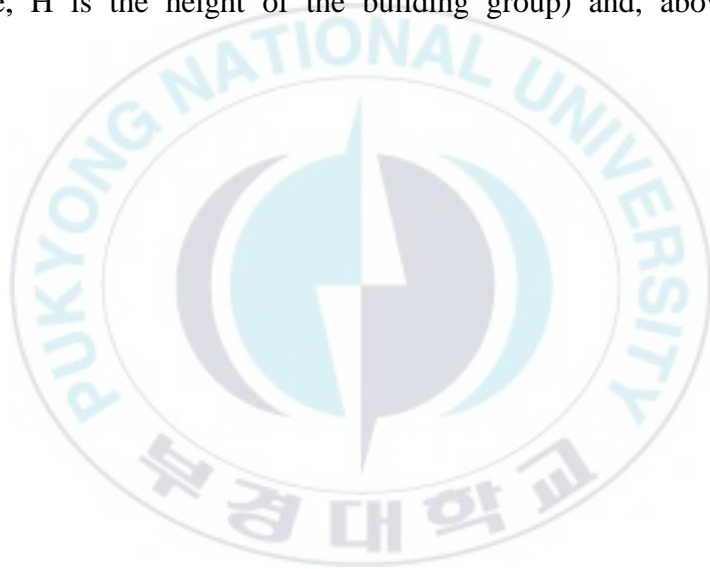
### **3.1. Simplified building group**

#### **3.1.1. Analysis on the change region by building group**

In this chapter, the area changed by buildings is analyzed. The Figure 2a shows changed area that is reduced by more than 10% compared to initial inflow profile on the component (u) in the x-direction. Although it is difficult to quantitatively define the influence range of flow by building group, the influent range of flow is defined to regions where are decreased by more than 10 % compared to initial inflow profile on the u-component in this study (Fig. 4).

EXP1 which has the smallest volumetric ratio is the smallest area affected. As the volumetric ratio of building group increases, the area affected is widen in the form of a logarithmic function (Fig. 5a). This result consistent with preceding research refers to the fact that affects widen area as volume building group increases (Lee et al., 2009). Also, it suggests that the domain

design of numerical experiments is determined on the basis of the recommended conditions of COST to eliminate the boundary effect. In vertical affected area by building group in Figure 5b, in the control case, the area affected by building is the most small in lower level than building height but the effects reveal to high level than other case. The wind speed reduced area rather decreases with the volumetric ratio near the ground bottom ( $z \lesssim 0.7H$ , here,  $H$  is the height of the building group) and, above  $0.7H$ , it increases.



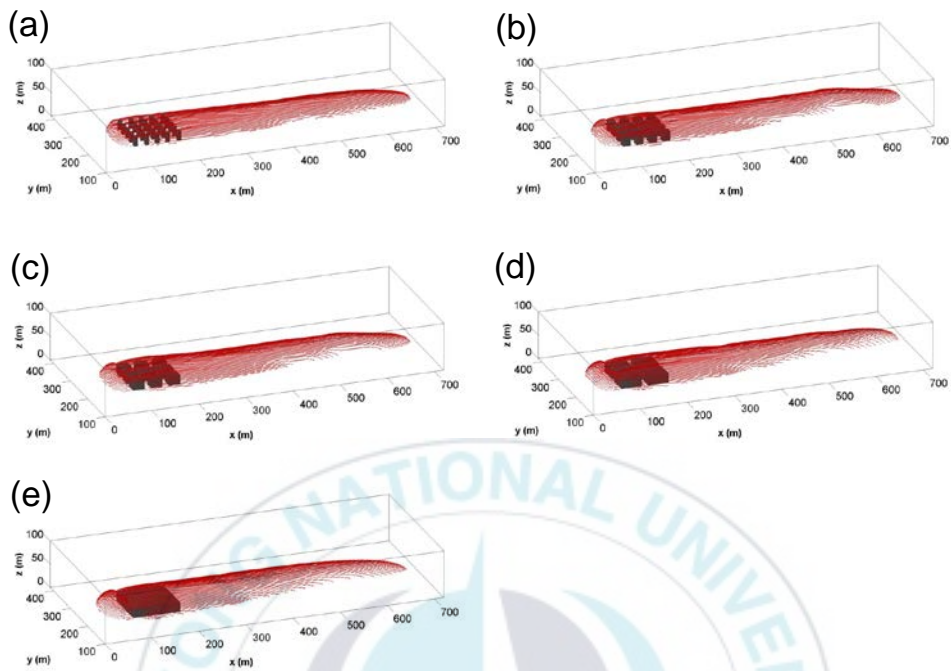


**Fig. 4.** Isosurface for the 10% reduction region of wind component in the x-direction (U) in each case.

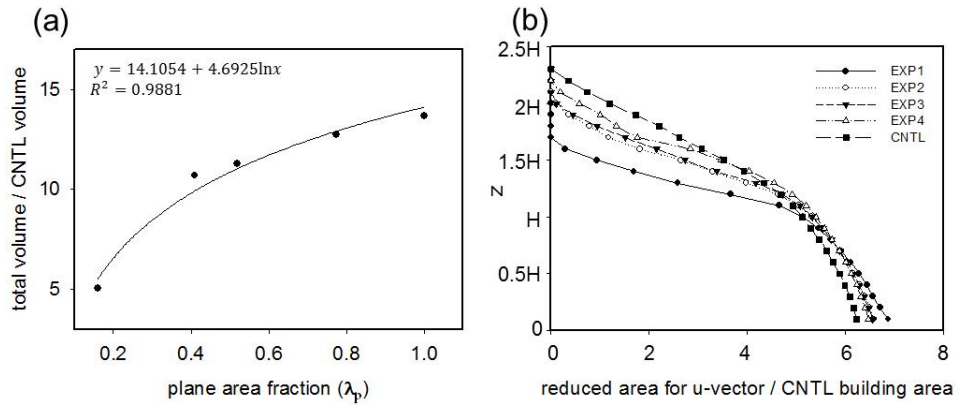


**Fig. 5.** (a) total volume of the reduction region in U-vector normalized by the building volume in the CNTL case and (b) U-vector reduced area fraction normalized by the plane area of the building in the CNTL case.

### 3.1.2. Parameterization for wind speed within building group

Figure 6 shows averaged vertical profiles of the wind speed within the buildings. As the volumetric ratio of the building group increases, the averaged wind speed within the buildings decreases. Because the friction by buildings increases as the volumetric ratio of building group increases. Wind speed within buildings is reduced compared with background flow due to friction effect by buildings. These effects do not reflected in mesoscale meteorological model, it is over estimated in urban area (Byon *et al.*, 2010).

In this study, it is investigated whether the wind speed within building group and wind speed of background are significantly associated with building volume. The averaged wind speed decreased non-linearly, as the volume of building increases and inflow wind speed decreases (Fig. 7). Based on the referred information, inside the building group, wind speed decreased with the volumetric ratio and averaged wind speed is parameterized in terms of the volumetric ratio and background flow speed. After that, the parameterized equation is compared with results obtained by numerically simulating in real urban areas. For this, it is assumed that the averaged wind speed can be expressed in combination of function for plane area fraction of buildings and initial inflow as eq (11). When the inflow wind

speed is constant,  $f$  is calculated by regression analysis. And then, when the plane area fraction of buildings is constant,  $g$  is calculated in the same method. The averaged wind speed within building group parametrized through these process is shown in eq (11)—(13).

$$U_p = f(\lambda_p) / g(U_h) \quad (11)$$

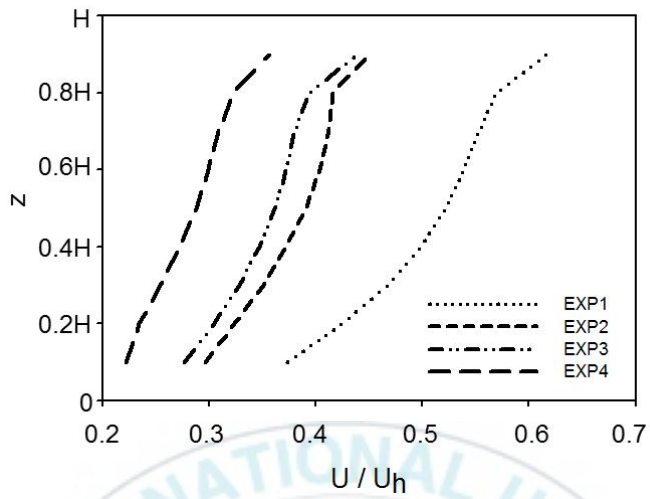
$$f(\lambda_p) = -1.1852\lambda_p^3 + 1.8754\lambda_p^2 - 1.1857\lambda_p + 0.5315 \quad (12)$$

$$g(U_h) = -0.0008U_h^4 + 0.017U_h^3 - 0.1261U_h^2 + 0.3009U_h + 0.7786 \quad (13)$$

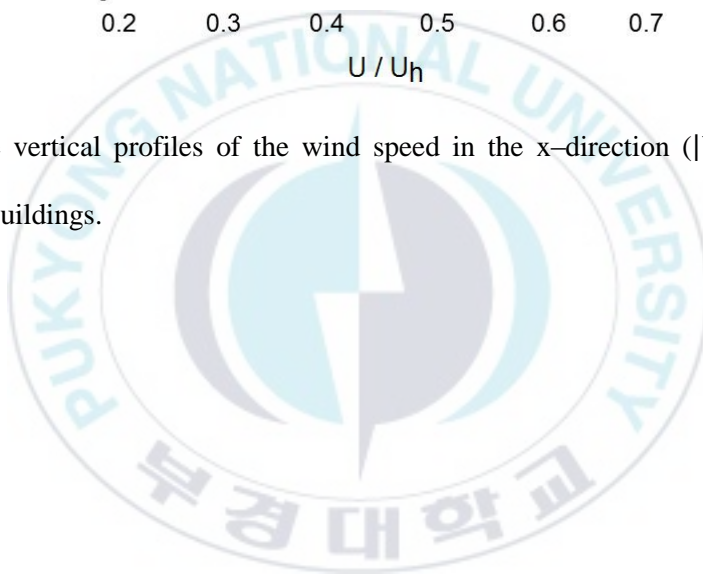
For the verification of this formula, the parameterized method is applied to 80 urban areas in 7 cities (Seoul, Busan, Deagu, Gwangju, Daejeon, Ulsan, Jeonju) in Korea. Figure 8 shows the averaged wind speed in urban areas by using parameterized method and simulation of CFD model, respectively. As a result of comparing the averaged wind speed within building group, the method developed in this study is relatively well parameterize the averaged wind speed in urban areas as  $R^2 = 0.69$ . But, the wind speed calculated in the parameterized method shows tendency of overestimation about  $0.1 \sim 0.2 \text{ m s}^{-1}$  than wind speed obtained by simulation with CFD model. Also, low value of wind speed such as less than  $0.3 \text{ m s}^{-1}$  could not be calculated. It is determined that the limitation of these results because it does not take into

account changes in height and frontal area fraction of buildings and it is considered only case where the building is regularly arranged in this experiment. Therefore, there is necessary to compensate parametrization scheme through systematic method by considering different height and array of buildings in the future.





**Fig. 6.** The vertical profiles of the wind speed in the x-direction ( $|U|$ ) averaged within the buildings.



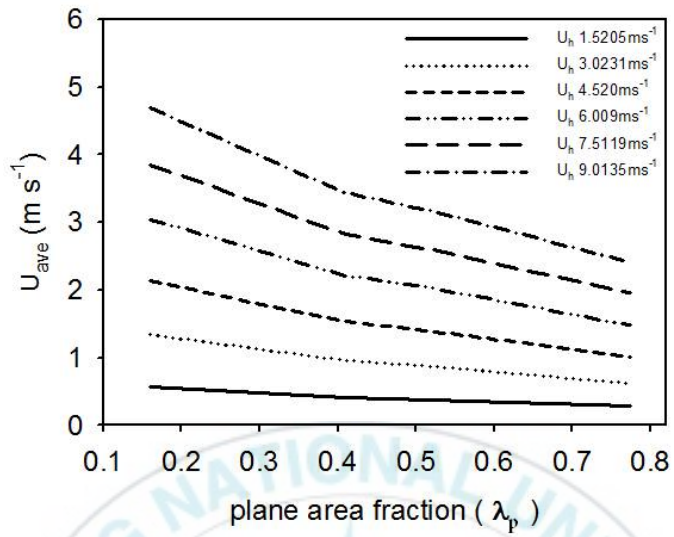


**Fig. 7.** The wind speed averaged within the buildings with the inflow speed and plane area fraction ( $\lambda_p$ ).

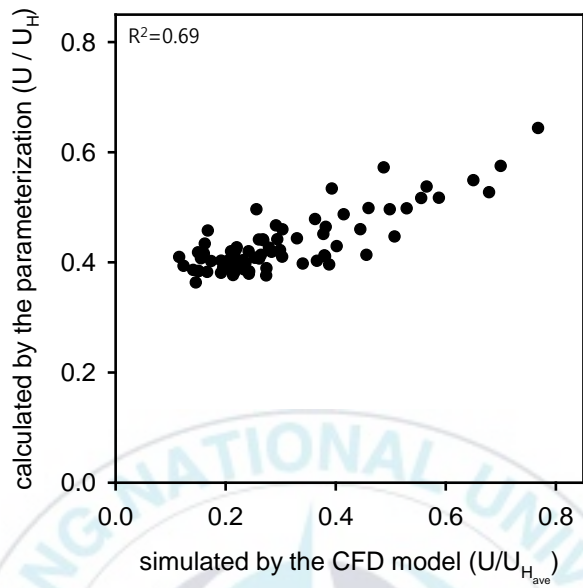


**Fig. 8.** Wind speed calculated by the parameterization method versus simulated by the CFD model using GIS data for 80 target areas selected in 7 cities in Korea.

## 3.2. Real area

### 3.2.1. Correlations between bulk geometric parameters and wind speed

It is possible derivation of parameters that can reflect the effect of buildings on mesoscale meteorological model because the shape and height of buildings are diverse in real urban area. For this, it is necessary to know the different bulk geometric parameters of buildings in real urban area. Bulk geometric parameters considered in this study include the average building height ( $H_{ave}$ ), maximum building height ( $H_{max}$ ), standard deviation of building height ( $\sigma_H$ ), plane area fraction of buildings ( $\lambda_p$ ), frontal area fraction of buildings ( $\lambda_f$ ) (Macdonald *et al.*, 1998). Also, the volumetric ratio of buildings ( $\lambda_{vol}$ ) is analyzed in this study.  $\lambda_p$  is defined as the ratio of the plane area occupied by buildings to plane area of the numerical domain.  $\lambda_f$  is defined as the ratio of the frontal area of buildings to plane area of the numerical domain. First of all, for the 120 districts, correlations among bulk geometric parameters ( $H_{ave}$ ,  $H_{max}$ ,  $\sigma_H$ ,  $\lambda_p$ , and  $\lambda_f$ ) are analyzed. Kanda *et al.* (2013) reported that, despite theoretical independency among the geometric parameters, there are significant correlations among them. The results in this study show that  $H_{ave}$  and  $H_{max}$  are well correlated with  $\sigma_H$  (Figs. 9a and 9b).

However, in Figure 9c,  $\lambda_p$  shows relatively poor correlation with  $\lambda_f$  in this analysis despite  $\lambda_p$  and  $\lambda_f$  have high positive correlation in preceding research (Kanda *et al.*, 2013). The reason for this is that target area in this analysis includes housing and plant areas. The area with small plane area fraction ( $\lambda_p < 0.2$ ) can be referred to nonurban area (Kanda *et al.*, 2013) and analysis of correlation between  $\lambda_p$  and  $\lambda_f$  gives an insight for characterizing urban types. It is possible to grasp the type of buildings in target area from correlation of  $\lambda_p$  and  $\lambda_f$ . The buildings of target areas excluding grey zone mean that as height is high, plane area is large. These areas include commercial or apartment area. The grey zone means that the target areas have districts such as housing and plant which are occupied of relatively low height and large plane area. Synthetically, all districts can be classified into three types. If  $\lambda_f$  is greater than  $\lambda_p$ , in the case of  $\lambda_p \geq 0.2$ , the regions mostly include commercial and apartment area. On the other hand, if  $\lambda_f$  is less than  $\lambda_p$ , the regions mostly include residential, industrial area. In the case of  $\lambda_p < 0.2$ , the regions are non-urban area. On the basis of results, bulk geometric parameters like  $\lambda_p$  and  $\lambda_f$  reflect well types of urban.

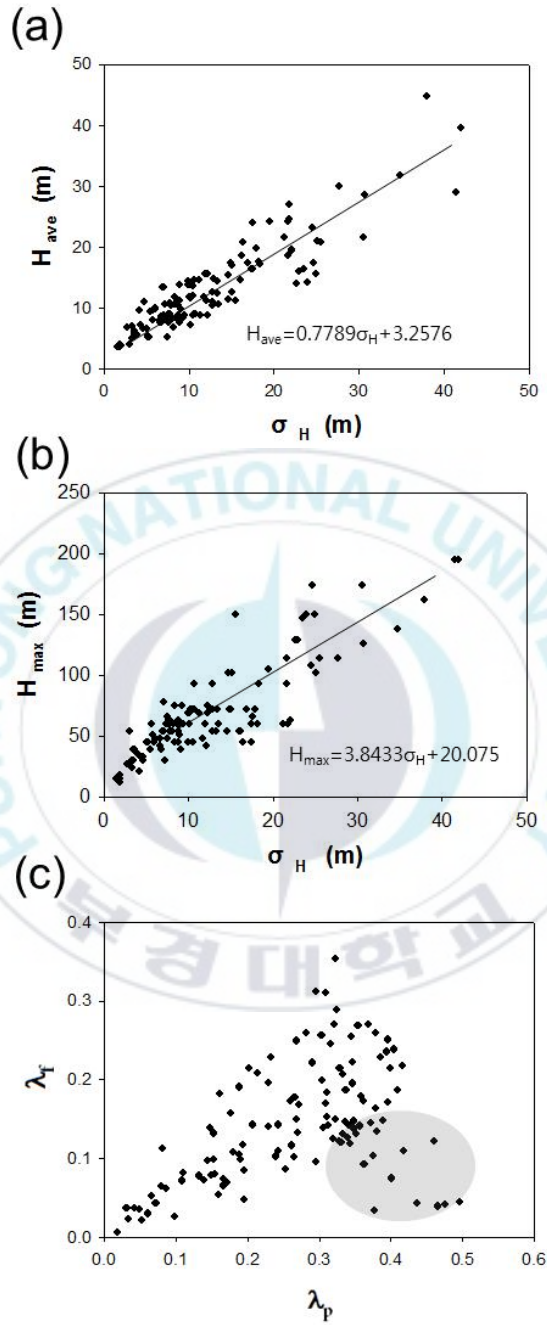


**Fig. 9.** The correlation between (a)  $\sigma_H$  and  $H_{ave}$ , (b)  $\sigma_H$  and  $H_{max}$ , (c)  $\lambda_f$  and  $\lambda_p$ .

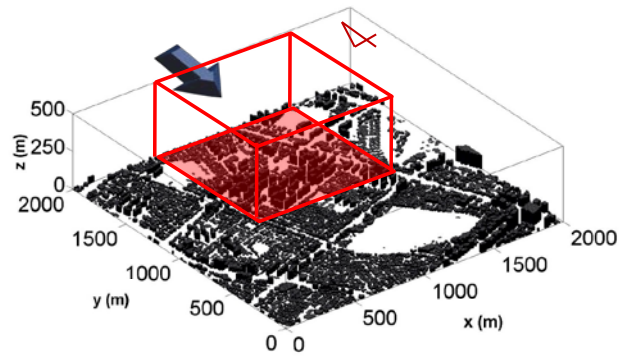
Changes in wind speed due to buildings are investigated by using CFD model. As mentioned in Chapter 2, 30 areas and 4 inflow directions for each area are considered. To see how wind speed can be affected by buildings, wind speed in the central area is compared with inflow speed. Figure 10 shows the variation of wind speed at a representative district (north section of gang-nam in Seoul). When initial flow direction is  $0^\circ$ , there is change in the averaged wind speed for x-(west-east) direction at  $z = 2.5$  m (the lowest layer of target area) as seen from the y-(south-north) direction. Wind speed in lower layer is reduced as building height is high. It means a decrease in wind speed due to influence of buildings.

Totally 120 districts are analyzed for change of wind speed with  $H_{ave}$ ,  $H_{max}$ ,  $\lambda_p$  and  $\lambda_f$ . As seen in Figure 11, there is little change in wind speed at  $z = 195.0$  m (the tallest building height of 120 districts) but wind speed at  $z = 12.5$  m (the average building height of 120 districts) is significantly changed as value of building parameters. It means that reduction of wind speed is influenced by buildings in lower layer where building is located.  $H_{ave}$  and  $H_{max}$  with wind speed have negative correlation, but the values of R is lower than 0.5 ( $H_{ave} : R = -0.3930$ ,  $H_{max} : R = -0.4406$ ). Although the average and maximum height of building are able to show the trend of wind speed reduction, it does not represent significant correlation. The  $\lambda_p$  is not to

represent certain correlation with wind speed. As value of  $\lambda_p$  is very high, reduction of wind speed is not appear large since target area include the buildings which is relatively low height and large area. On the other hand, wind speed at  $z = 12.5$  m is decreased as  $\lambda_f$  is increased and the reduction in wind speed is strongly related with  $\lambda_f$  of building ( $R = -0.8227$ ). It can be known  $\lambda_f$  is critical factor that well reflects to effect of building for reduction of wind speed.



(a)



(b)

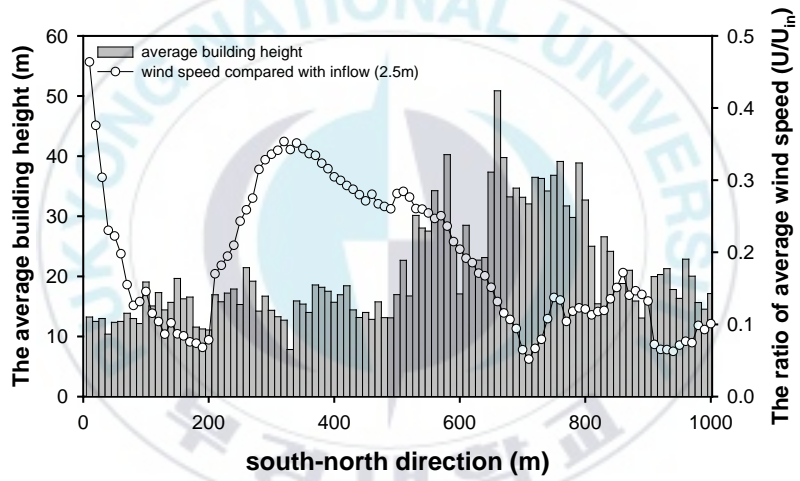


**Fig. 10.** (a) The domain of gang-nam in Seoul and (b) the variation of wind speed at  $z = 2.5$  m with building height.

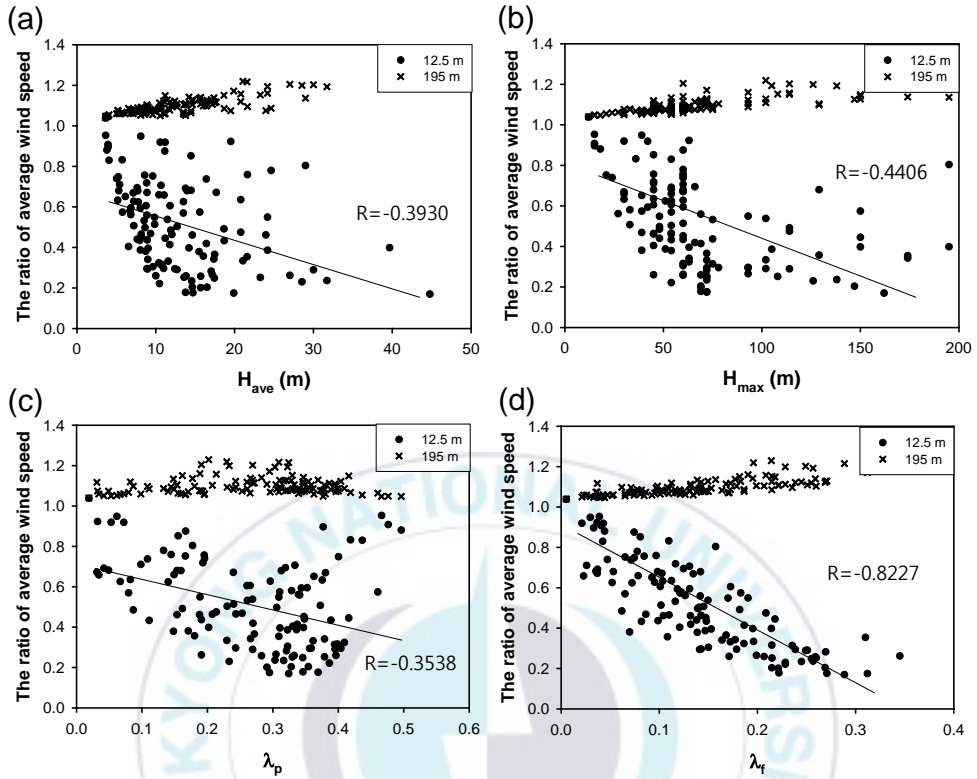


**Fig. 11.** The ratio of average wind speed at 12.5 m and 195.0 m over the central area to inflow speed with (a)  $H_{ave}$ , (b)  $H_{max}$ , (c)  $\lambda_p$  and (d)  $\lambda_f$ . The average building height of 120 districts is 12.5 m and the tallest building height considered in this study is 195.0 m.

### 3.2.2. Roughness length and zero plane displacement height

Roughness length ( $z_0$ ) is related directly to the surface drag and it represents well the characteristics of surface.  $z_0$  can be typically estimated from bulk geometric parameters in urban area (Macdonald *et al.*, 1998). The zero plane displacement height ( $d$ ) is the appropriate reference level between the actual ground and the tops of roughness elements (Arya, 2001). In other words, it is regarded as the level at which mean drag appears on surface (Jackson, 1981). As the  $d$  is expected to increase with increasing roughness factors, it is larger in urban areas than non-urban areas because of buildings (Arya, 2001). In accordance with these reasons, roughness length and zero plane displacement height are important indicators in urban. Here we estimated the value of  $z_0$  and  $d$  for the 120 districts by following formulas proposed by Kanda *et al.* (2013).

$$\frac{z_0}{z_0(\text{mac})} = b_1 Y^2 + c_1 Y + a_1, \quad Y = \frac{\lambda_p \sigma_H}{H_{ave}} \quad (14)$$

$$\frac{d}{H_{max}} = c_0 X^2 + (a_0 \lambda_p^{b_0} - c_0) X, \quad X = \frac{\sigma_H + H_{ave}}{H_{max}} \quad (15)$$

Where  $a_0$  (= 1.29),  $b_0$  (= 0.36),  $c_0$  (= -0.17),  $a_1$  (= 0.71),  $b_1$  (= 20.21)

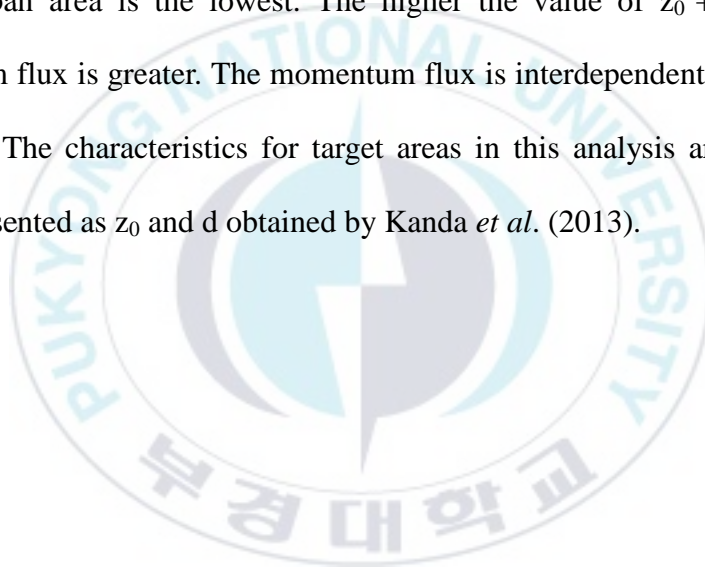
and  $c_1$  ( $= -0.77$ ) are constant parameters (Kanda *et al.*, 2013).  $z_0$  (mac) is roughness length calculated by Macdonald *et al.* (1998). The method was enhanced to recreate these roughness parameters (Kanda *et al.*, 2013).

By taking into account zero plane displacement height for buildings in urban, the effective roughness height ( $z_0 + d$ ) is proper to reflect the characteristics of real urban (Grimmond and Oke, 1999, Gross, 2014) (Fig. 12). For that reason, in this study, it should be analyzed for value of  $z_0 + d$ . In consideration of zero plane displacement height, the  $z_0 + d$  rather than simple roughness length ( $z_0$ ) express well changes on the wind profile by buildings in urban (Gross, 2014). Figure 13 shows vertical average momentum flux ( $\tau$ ) and height of  $z_0 + d$  for each district depending on the type of urban classification in chapter 3.1. The momentum flux is calculated by following formula.

$$\tau = \rho K_m \left( \frac{\partial U}{\partial z} \right) \quad (16)$$

$\rho$ ,  $K_m$  are air density and eddy viscosity, respectively (Arya, 2001). The distribution of high buildings in urban surface induces loss of momentum with frictional force (Martilli *at el.*, 2002). Flux is used for application of variables within urban in mesoscale model (Chen *et al.*, 2004).

Radiant flux of surface is expressed by calculating momentum, sensible heat, latent heat, soil heat and so on. In this study, momentum flux is obtained by calculating eddy viscosity and vertical wind speed profile using CFD model (Arya, 2001). The greatest loss of momentum flux is appeared in the districts consists of commercial and apartment area. In residential and industrial areas, momentum flux had lost at relatively low level. The loss of momentum flux in non-urban area is the lowest. The higher the value of  $z_0 + d$ , loss of momentum flux is greater. The momentum flux is interdependent with height of  $z_0 + d$ . The characteristics for target areas in this analysis are generally well represented as  $z_0$  and  $d$  obtained by Kanda *et al.* (2013).



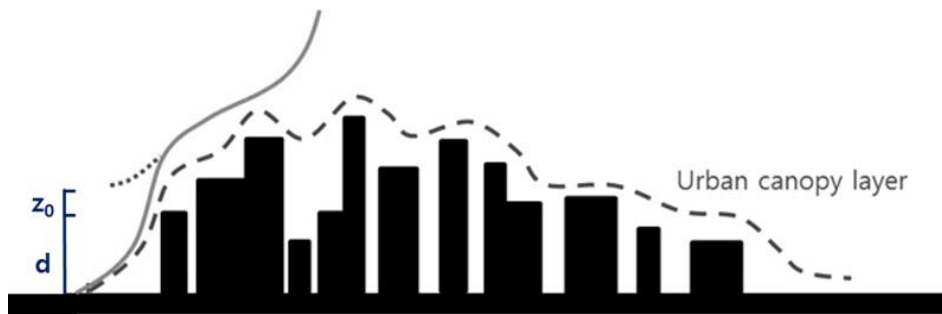


**Fig. 12.** The roughness length ( $z_0$ ) and zero plane displacement height ( $d$ ) of urban canopy layer.



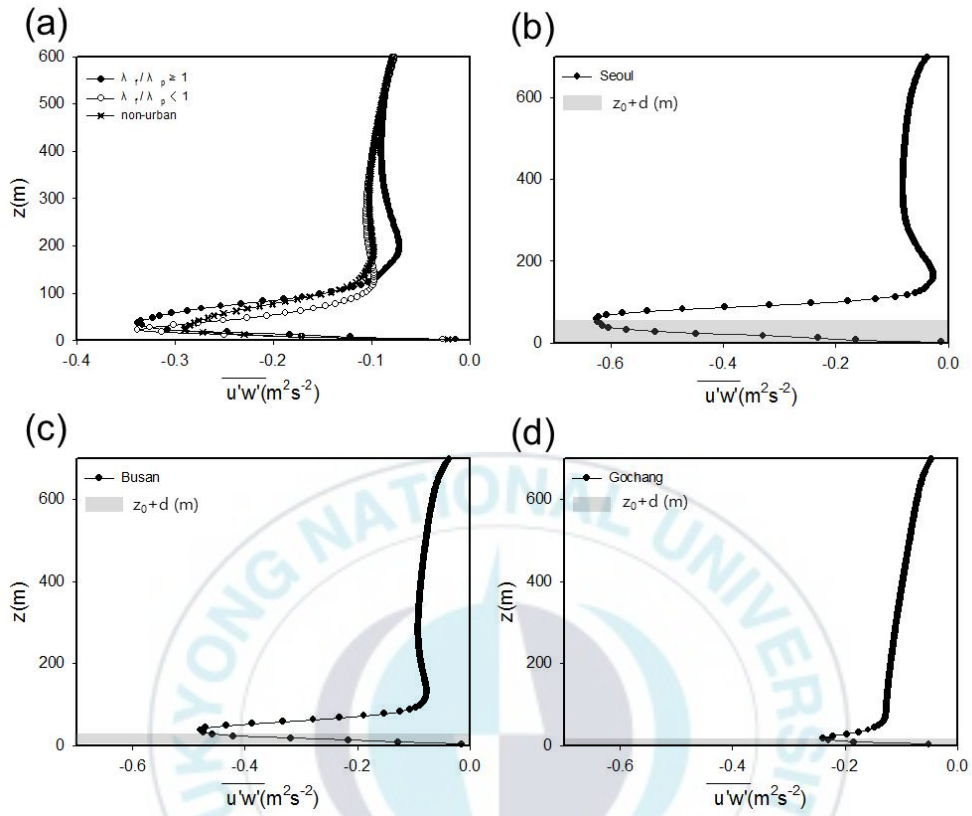


**Fig. 13.** Vertical average momentum flux and effective roughness height for three urban type. The averaged momentum flux (a) and Seoul (b), Busan (c), Gochang (d) as representative area of each type.

### 3.2.3. The correlation among effective roughness height and bulk geometric parameters

The bulk geometric parameters are analyzed to derive new parameter that can be simply alternative for the effective roughness height. Calculated roughness length and zero plane displacement height are shown in Figure 14. The zero plane displacement height and displacement height show rather a parabolic variation with  $\lambda_p$ . Two parameters increase with  $\lambda_p$  for small  $\lambda_p$  ( $< 0.25$ ) and then, it decrease. These parameters do not show clear correlation and these results mean  $\lambda_p$  does not seem to be enough to explain roughness height. When  $\lambda_f$  which is most relevant with wind speed reduction by building is analyzed with roughness length and zero displacement height, they show positive correlation respectively. But, although the roughness length and zero plane displacement height are affected by  $\lambda_f$  as effect for the geometrical shape of buildings,  $\lambda_f$  is not possible to accurately represent the roughness elements as  $R^2 = 0.3908$  and  $R^2 = 0.4627$ , respectively. We analyzed volume ratio ( $\lambda_{vol}$ ) of building from bulk geometric parameters and the roughness length and zero plane displacement height. The volumetric ratio is possible to reflect both of  $\lambda_p$  and  $\lambda_f$ . Figure 15 shows correlations of the roughness length and displacement height respectively with volumetric

ratio ( $\lambda_{vol}$ ) of buildings for the total 120 districts. The value for ratio of volume represents better roughness elements clearly as  $R^2 = 0.7203$  and  $R^2 = 0.7731$ , respectively. The following formula is the regression equation associated therewith.

$$\frac{z_0}{H_{ave}} = 432.25 \lambda_{vol}^2 + 50.537 \lambda_{vol} - 0.0807 \quad (17)$$

$$\frac{d}{H_{ave}} = 808.1 \lambda_{vol}^2 + 192.35 \lambda_{vol} + 0.3901 \quad (18)$$

By using these equations, Roughness length and zero plane displacement height can be simply estimated by using  $\lambda_{vol}$ . It is convenient to obtain volumetric ratio than  $\lambda_f$  calculated depending on inflow direction of each in model. It is determined that parameters by using volumetric ratio of building can be easily applied to mesoscale meteorological model in the future.

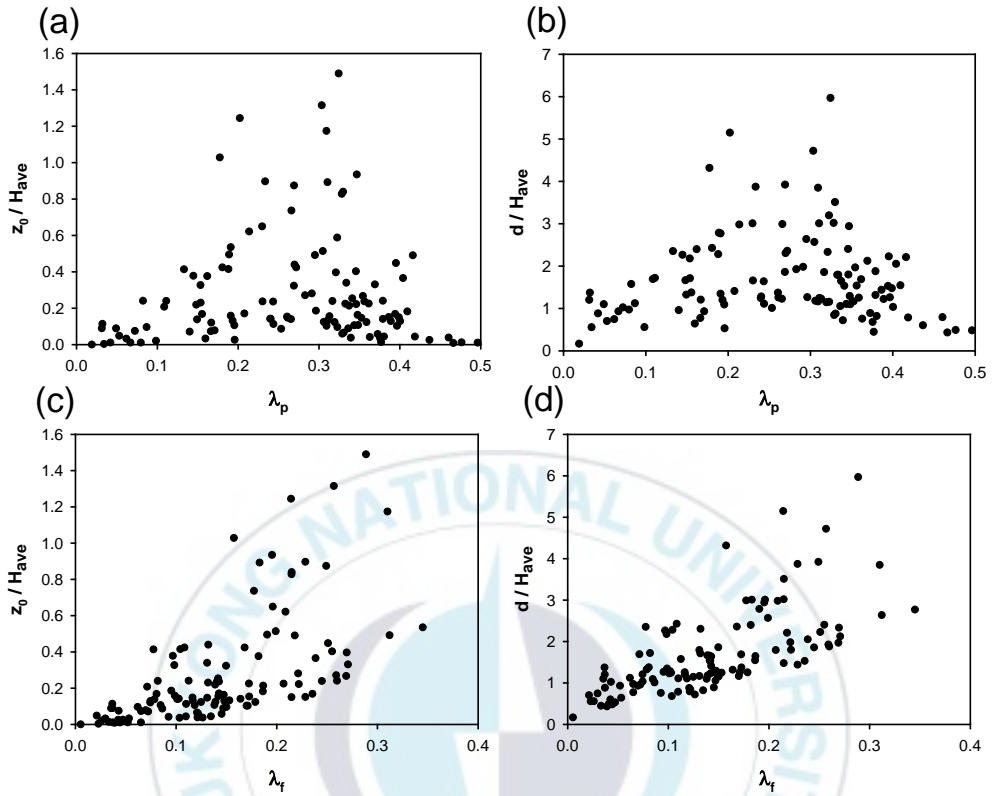


**Fig. 14.** The correlation between (a)  $z_0$  and  $\lambda_p$ , (b)  $d$  and  $\lambda_p$ , (c)  $z_0$  and  $\lambda_f$ , (d)  $d$  and  $\lambda_f$ .

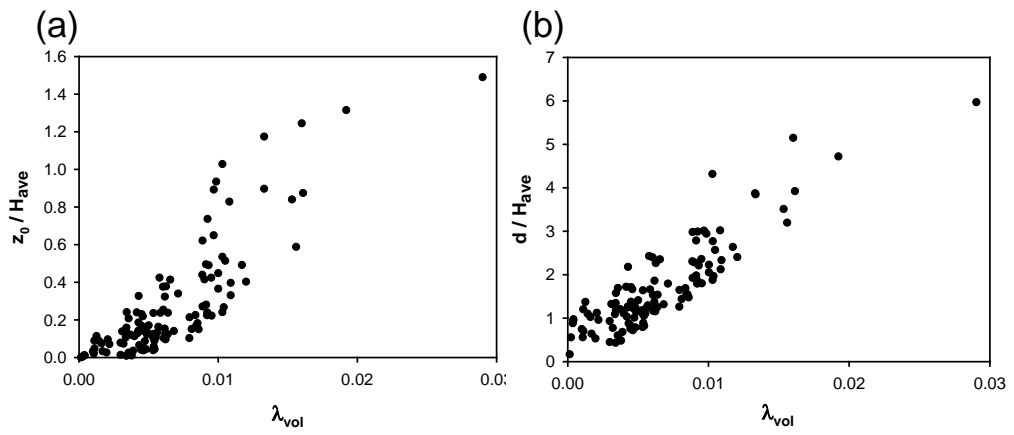
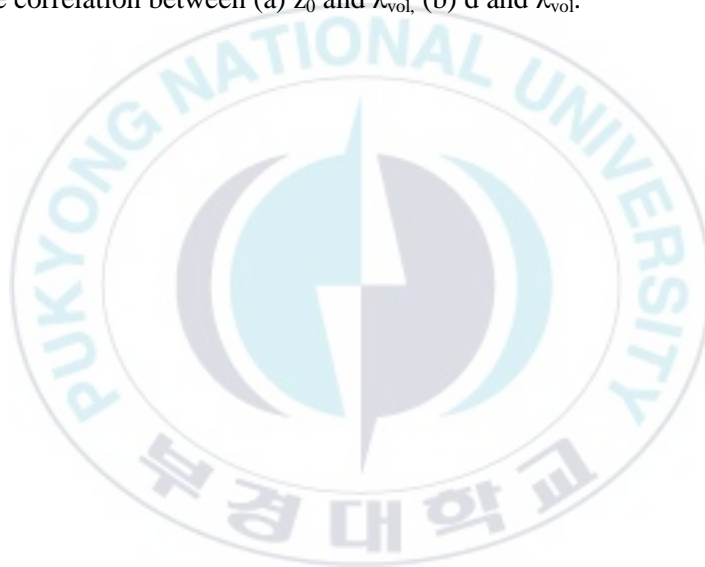


**Fig. 15.** The correlation between (a)  $z_0$  and  $\lambda_{vol}$ , (b)  $d$  and  $\lambda_{vol}$ .



## 4. Summary and conclusions

In this paper, two experiments were analyzed. In the first study, the characteristics of flows around building group were investigated. For this, uniformly arrayed building group with different volumetric ratios in a fixed area was considered. As the volumetric ratio of the building group increases, the region affected by the building group was widened. However, the wind-speed reduced area rather decreases with the volumetric ratio near the ground bottom ( $z \lesssim 0.7H$ , here,  $H$  is the height of the building group) and, above  $0.7H$ , it increased. Inside the building group, wind speed decreased with the volumetric ratio and averaged wind speed was parameterized in terms of the volumetric ratio and background flow speed. The parameterization method was applied to producing averaged wind speed for 80 urban areas in 7 cities in Korea, showing relatively good performance. But, the results from parameterization method were a little over estimated than results from CFD simulation and could not calculate low value. Therefore, there is necessary to compensate parametrization scheme through systematic method by considering different height and array of buildings in the future because

limitation by uniformly arrayed buildings is showed in this analysis.

In the second study, we analyzed urban parameterizations that are possible to apply to mesoscale meteorological model. For this, to analyze the effects of building, real 120 target areas were considered. Bulk geometric parameters including the plane and frontal area fractions, average and maximum building heights, and standard deviation of building height were calculated from GIS data for the 120 target areas. Bulk geometric parameters had close correlation with each other. As a result, the 120 districts could classify into three types depending on  $\lambda_p$  and  $\lambda_f$ . The target areas in this study showed districts that have residential and plant areas. In CFD simulation results, the buildings resulted in decrease of wind speed at lower level.  $\lambda_f$  in the geometric parameters significantly affected to reduction of wind speed. Roughness length and zero plane displacement height were estimated based on the bulk geometric parameters. The roughness length and zero displacement height indicated height of the most loss for momentum flux from CFD simulation. Both of them have positive correlation with  $\lambda_f$ , but have not high value of  $R^2$ . The roughness length and zero displacement height present high correlation with volumetric ratio of building. As a result, those could be more easily estimated as only  $\lambda_{vol}$  in this analysis. It is determined that parameters by using volumetric ratio of building can be

applied to mesoscale meteorological model in the future. In mesoscale model, it is expected that the influence of buildings is possible to be effectively reflected in urban area.



## Reference

- Arya, S. P., 2001: Introduction to micrometeorology, 2nd Ed. Academic press, 204–211.
- Bhagat, R. B., 2005: RURAL-URBAN CLASSIFICATION AND MUNICIPAL GOVERNANCE IN INDIA. *Singapore Journal of Tropical Geography*, **26**, 61–73.
- Brown, M. J. and M. D. Williams, 1998: An urban canopy parameterization for mesoscale meteorological models. *Atmospheric Environment*, **30**, 413–427.
- Britter, R. E. and S. R. Hanna, 2003: Flow and dispersion in urban areas. *Annual Review of Fluid Mechanics*, **35**, 469–496.
- Byon, J. Y., Y. J. Choi and B. G. Seo, 2010: Evaluation of Urban Weather Forecast Using WRF-UCM (Urban Canopy Model) Over Seoul. *Atmosphere*, **20**(1), 13–26.
- Chen, F., H. Kusaka, M. Tewari, J.-W. Bao and H. Hirakuchi, 2004: Utilizing the coupled WRF/LSM/Urban modeling system with detailed urban classification to simulate the urban heat island phenomena over the Greater Houston area. *Fifth Symposium on the Urban Environment*, **2004**. 9–11
- Chu, A. K. M., R. C. W. Kwok and K. N. Yu, 2005: Study of pollution dispersion in urban areas using Computational Fluid Dynamics (CFD) and Geographic Information System (GIS). *Environmental Modelling & Software*, **20**, 273–277.

- Franke, J., A. Hellsten, K. H. Schlunzen and B. Carissimo, 2011: The COST 732 Best Practice Guideline for CFD simulation of flows in the urban environment: a summary. *International Journal of Environment and Pollution*, **44**, 419-427.
- Grimmond, C. S. B. and T.R. Oke, 1998: Aerodynamic properties of urban areas derived from analysis of surface form. *Journal of applied meteorology*, **38**, 1262–1292.
- Gross, G., 2014: On the Parametrization of Urban Land Use in Mesoscale Models. *Boundary-layer meteorology*, **150**, 319–326.
- Kanda, M., A. Inagaki, T. Miyamoto, M. Gryschka and S. Raasch, 2013: A new aerodynamic parametrization for real urban surfaces. *Boundary-layer meteorology*, **148(2)**, 357–377.
- Kastner-Klein, P., R. Berkowicz and R. Britter, 2004: The influence of street architecture on flow and dispersion in street canyons. *Meteorology and Atmospheric Physics*, **87**, 121–131.
- Kim, J. –J., 2007: The Effects of Obstacle Aspect Ratio on Surrounding Flows. *Atmosphere*. **17**, 381–391.
- \_\_\_\_\_, and J. –J. Baik, 2010: Effects of Street-Bottom and Building-Roof Heating on Flow in Three-Dimensional Street Canyons. *Atmosphere*. **27**, 513–527.
- \_\_\_\_\_, E. Pardyjak, D. Y. Kim, K. S. Han and B. H. Kwon, 2014: Effects of building-roof cooling on flow and air temperature in urban street canyons. *Asia-Pacific Journal of Atmospheric Sciences*, **50**, 365–375.

- Lee, J. H., J. W. Choi and J. -J. Kim, 2009: The Effects of an Urban Renewal Plan on Detailed Air Flows in an Urban Area. *Journal of the Korea Association of Geographic Information Studies*, **12**, 69–81.
- \_\_\_\_\_, M. Shahgedanova and K. White, 2009: The role of urban parameters in the development of urban heat island: analysis and statistical modelling. *The seventh International Conference on Urban Climate*. 29 June–3 July, Yokohama, Japan.
- Lee, S.-H., S.-W. Kim, W. M. Angevine, L. Bianco, S. A. McKeen, C. J. Senff, M. Trainer, S. C. Tucker, and R. J. Zamora, 2011: Evaluation of urban surface parameterizations in the WRF model using measurements during the Texas Air Quality Study 2006 field campaign. *Atmospheric Chemistry and Physics*, **11**, 2127–2143.
- Lu, D. and Q. Weng, 2006: Use of impervious surface in urban land-use classification. *Remote Sensing of Environment*, **102**, 146–160.
- Macdonald, R. W., R. F. Griffiths and D. J. Hall, 1998: An improved method for the estimation of surface roughness of obstacle arrays. *Atmospheric Environment*, **32**, 1857–1864.
- Martilli, A., A. Clappier and M. W. Rotach, 2002: An urban surface exchange parameterisation for mesoscale models. *Boundary-Layer Meteorol*, **104**, 261–304.
- Neofytou, P., M. Haakana, A. Venetsanos, A. Kousa, J. Bartzis and J. Kukkonen, 2008: Computational fluid dynamics modelling of the pollution dispersion

- and comparison with measurements in a street canyon in Helsinki. *Environmental Modeling & Assessment*, **13**, 439-448.
- Ohashi, Y., Y. Genchi, H. Kondo, Y. Kikegawa, H. Yoshikado and Y. Hirano, 2007: Influence of air-conditioning waste heat on air temperature in Tokyo during summer: numerical experiments using an urban canopy model coupled with a building energy model. *Journal of Applied Meteorology and climatology*, **46**, 66–81.
- Oke, T. R., 2006: Towards better scientific communication in urban climate. *Theoretical and Applied Climatology*, **84**, 179–190.
- Santiago, J. L., O. Coceal and A. Martilli, 2013: How to parametrize Urban-Canopy Drag to reproduce wind-direction effects within the canopy. *Boundary-Layer Meteorol*, **149**, 43–63.
- Tewari, M., F. Chen, H. Kusaka and S. Miao, 2008: Coupled WRF/Unified Noah/urban-canopy modeling system. *NCAR WRF Documentaton, NCAR, Boulder*, 1–20.
- Toparlar, Y., B. Blocken, P. Vos, G. J. F. van Heijst, W. D. Janssen, T. van Hooff, H. Montazeri and H. J. P. Timmermans, 2015: CFD simulation and validation of urban microclimate: A case study for Bergpolder Zuid, Rotterdam. *Building and Environment*, **83**, 79–90.
- Zheng, M. H., Y. R. Guo, X. Q. Ai, T. Qin, Q. Wang and J. M. Xu, 2010: Coupling GIS with CFD modeling to simulate urban pollutant dispersion. *Mechanic*

*Automation and Control Engineering (MACE), 2010 International Conference, 1785-1788.*

Burian S. J., N. Augustus, I. Jeyachandran and M.J. Brown, 2007: Development and assessment of the second generation National Building Statistics database. *Seventh Symposium on the Urban Environment , San Diego, CA,10–13 September, American Meteorological Society: Boston, MA, Paper 5.4.*

